Infection with CagA$^+$ *Helicobacter pylori* induces epithelial to mesenchymal transition in human cholangiocytes

Prissadee Thanaphongdecha[1,2,3], Shannon E. Karinshak[1], Wannaporn Ittiprasert[1], Victoria H. Mann[1], Yaovalux Chamgramol[3], Chawalit Pairojkul[3], Sutas Suttiprapa[2], Banchob Sripa [2,3,*], Paul J. Brindley[1,*]

[1] Department of Microbiology, Immunology and Tropical Medicine, and Research Center for Neglected Tropical Diseases of Poverty, School of Medicine & Health Sciences, The George Washington University, Washington DC, 20037, USA

[2] Tropical Disease Research Laboratory, Faculty of Medicine, Khon Kaen University, Khon Kaen 40002, Thailand

[3] Department of Pathology, Faculty of Medicine, Khon Kaen University, Khon Kaen, 40002, Thailand

[*] Equal contribution

Correspondence: Paul J. Brindley, Department of Microbiology, Immunology and Tropical Medicine, and Research Center for Neglected Tropical Diseases of Poverty, School of Medicine & Health Sciences, The George Washington University, Washington DC, 20037, USA, email, pbrindley@gwu.edu; or Banchob Sripa, Tropical Disease Research Laboratory, Department of Pathology, Faculty of Medicine, Khon Kaen University, Khon Kaen 40002, Thailand, email, banchob@kku.ac.th

Abstract

Recent reports suggest that the East Asian liver fluke *Opisthorchis viverrini*, which is implicated in pathogenesis of opisthorchiasis-associated cholangiocarcinoma, serves as a reservoir of *Helicobacter pylori*. The affected cholangiocytes that line the intrahepatic biliary tract are considered to be the cell of origin of this malignancy. Here, we investigated interactions among a human cholangiocyte cell line, H69, a CCA cell line CC-LP-1, CagA^{+}ve *Helicobacter pylori*, and *H. bilis* bacilli. Exposure to increasing numbers of *H. pylori* at 0, 1, 10,100 bacteria per H69 cell for 24 hrs induced phenotypic changes in the cultured cholangiocytes including profusion of thread-like filopodia and loss of cell-cell contact in a dose-dependent fashion. In parallel, changes in mRNA expression followed exposure to *H. pylori*, with increased expression of epithelial to mesenchymal transition (EMT) associated-factors including snail, slug, vimentin, matrix metalloprotease, zinc finger E-box-binding homeobox, and the cancer stem cell marker CD44. Transcription levels encoding the cell adhesion marker CD24 decreased. Analysis in real time using the xCELLigence system to quantify cell proliferation, migration and invasion revealed that exposure to 10 to 50 of *H. pylori* stimulated migration of H69 cells and CC-LP-1 cells, a line derived form of a human cholangiocarcinoma, and invasion through an extracellular matrix. In addition, 10 bacilli of CagA^{+}ve *H. pylori*, but not *H. bilis*, stimulated contact-independent colony establishment in soft agar. These findings support the hypothesis that infection with *H. pylori* can contribute to the malignant transformation of the biliary epithelium.

Keyword : *Helicobacter pylori*, cholangiocyte, epithelial-to-mesenchymal transition.

Introduction

Complex associations occur between trematodes and bacterial commensals, including species capable of causing human diseases such as non-typhoidal salmonellosis, leptospirosis and Sennetsu fevers (1-3). There is increasing evidence that the East Asian liver fluke *Opisthorchis viverrini* may serve as a reservoir of *Helicobacter* and implicate *Helicobacter* in pathogenesis of opisthorchiasis-associated cholangiocarcinoma (CCA) (4-8). The International Agency for Research on Cancer of the World Health Organization classifies infection with the liver flukes *O. viverrini* and *Clonorchis sinensis* and with *H. pylori* as Group 1 carcinogens (9). In northern and northeastern Thailand and Laos, infection with *O. viverrini* is the major risk for CCA (9-12). Given the elevated prevalence of CCA in this region where infection with liver fluke prevails, and given evidence of linkages between human infection by *Helicobacter* during opisthorchiasis, these two biological carcinogens together may orchestrate the pathogenesis of opisthorchiasis and bile duct cancer. The association of *Helicobacter* and its virulence factors, including during opisthorchiasis, may underlie biliary tract disease including CCA in liver fluke-endemic regions (13). Infection with species of *Helicobacter* causes hepatobiliary tract diseases that can resemble opisthorchiasis (8, 14, 15) (16, 17). Lesions ascribed to liver fluke infection, including cholangitis, biliary hyperplasia and metaplasia, periductal fibrosis and CCA, may be due in part to *Helicobacter*-associated hepatobiliary disease.

Commensalism involving *H. pylori* and *O. viverrini* may have evolved and may facilitate conveyance of the bacillus into the human biliary tract during the migration of the juvenile fluke following ingestion of the metacercaria in raw or undercooked cyprinid fish and establishment of infection (4, 18). Since we have shown previously that curved rods resembling *Helicobacter* occur in the alimentary tract of the liver fluke (4), and given the low pH of the gut of *O. viverrini*, the *H. pylori* rods or spores might be transported by the migrating parasite. The spiral shape of *H. pylori* attach to biliary cells, which internalize in similar fashion to their behavior on gastric epithelium (19, 20).

Transition of epithelial cells to mesenchymal cells during disease and epithelial to mesenchymal transition (EMT) during development and wound healing follows conserved EMT routes with well-characterized molecular and morphological hallmarks (21). These hallmarks are clearly displayed at malignant transformation of the epithelium of the gastric mucosa resulting from infection with *H. pylori* (22). Here, we investigated interactions between CagA$^+$ve *H. pylori*, the related species *H. bilis* (23), and human cholangiocytes including the H69 cholangiocyte cell line (24, 25) and the CCLP-1cholangiocarcinoma cell line (26). Infection with CagA$^+$ *H. pylori* induced epithelial to mesenchymal transition in human cholangiocytes.

Materials and Methods

Human cholangiocyte lines

The immortalized intrahepatic cholangiocyte cell line, H69 (24, 25), Cellosaurus (27) identifier RRID:CVCL_812,1, and the primary cholangiocarcinoma cell line, CC-LP-1 (26, 28) Cellosaurus RRID CVCL_0205, were obtained as described (26, 28-30). In brief, H69 cells were cultured in Dulbecco's Modified Eagle's Medium (DMEM) (Thermo Fisher Scientific, Inc.),

139 DMEM/F12 (Sigma, St Louis) supplemented with 10% fetal bovine serum (FBS; Invitrogen;
140 Thermo Fisher Scientific, Inc.), supplemented with adenine, insulin, epinephrine,
141 triiodothyronine/transferrin, hydrocortisone and epidermal growth factor and
142 penicillin/streptomycin (PS). CC-LP-1 cells were cultured in DMEM containing 10%FBS, L-
143 glutamine and antibiotics as above. All cells maintained in humidified 5% CO_2 in air at 37°C.
144 The cells were cultured to ~80% confluence before co-culture with bacteria.
145
146 ***Helicobacter pylori* and *Helicobacter bilis***
147
148 *Helicobacter pylori*, ATCC 43504, isolated originally from human gastric antrum (31) and *H.*
149 *bilis*, Fox *et al.* ATCC 49314, originally isolated from intestines and liver of mice (32, 33), were
150 obtained from the American Type Culture Collection (ATCC) (Manassas, VA) and a gift from
151 Dr. Fox MIT and maintained on trypticase soy agar with 5% sheep blood for 72 to 96 hours (34)
152 (Becton Dickinson, Cockeysville, MD), incubated at 37°C with rocking under microaerobic
153 conditions with the BBL Campy Pack Plus system (Becton Dickinson). After 96 hours, each
154 bacterial species was harvested independently by scraping the colonies from the agar plate, the
155 cell scraping was resuspended in DMEM/F12 medium to an optical density at 600 nm (OD_{600}) of
156 1. 0 corresponding to approximately 1×10^8 colony forming units (cfu)/ml (35-37).
157
158 **Morphological assessment of cholangiocytes**
159
160 *H. pylori* was co-cultured with H69 cells at different multiplicities of infection (MOIs) of 0, 10
161 and 100 for 24 hours in serum-free media. After 24 hours, the effect of *H. pylori* to H69 cell
162 morphology were observed under an inverted microscope (Zeiss Axio Observer A.1) (Figure 1).
163
164 ***In vitro* wound healing assay**
165
166 Monitoring cell migration in a two-dimensional confluent monolayer in controlled *in vitro*
167 conditions allowed investigators to simulate and explore critical mechanisms of the impact of *H.*
168 *pylori* on the process of wound healing. Sheet migration (38, 39) was used in this study to
169 observe H69 cell migration after *H. pylori* exposure using differing MOI of 0, 10 or 100.
170 Briefly, H69 cells were grown in 6-well plates (Greiner, Monroe NC) overnight to allow cell
171 adherence. A linear thin scratch (wound) was created to produce a gap in the confluent cell
172 monolayer using a sterile 20 µl pipette tip. The gap was observed and measured for up to 26
173 hours. The gap width was analyzed using ImageJ software (NIH, USA). The wound closure rate
174 over time was calculated and compared with control group (H69 cells grown in the absence of *H.*
175 *pylori*). The statistical significance was analyzed by One-way ANOVA (Prism).
176
177 **Real time quantitative PCR (RT-qPCR) analysis**
178
179 Total RNA from H69 cells were extracted with RNAzol^{RT} (Molecular Research Center, Inc.)
180 according to the manufacturer's instructions. The RNA quality and concentration were assessed
181 using the NanoDrop 1000 spectrophotometer (Thermo Fisher Scientific, MA). Total RNA (500
182 ng) was reversed-transcribed using iScript cDNA Synthesis Kit (Bio-Rad, Hercules, CA).
183 Quantitative reverse transcription-polymerase chain reaction (qRT-PCR) analysis of mRNA
184 expression of six members of the EMT-associated genes including Vimentin, Snai1, Slug, Zeb,

185 Jam1 and MMP7; two cancer stem cells including CD44 and CD24 were undertaken on an
186 ABI7300 system (ABI) using SsoAdvance SYBR green mixture (Bio-Rad), normalized to
187 human GAPDH (Supplementary Table 1 provides the primer sequences). The relative fold-
188 change was determined by the ΔΔCt method (40). Three biological replicates of these assays
189 were carried out.
190
191 **Cell migration after *H. pylori* co-culture**
192
193 To monitor cell migration/invasion in real time, we used the xCELLigence Real-time cell
194 analyzer (RTCA) DP instrument (ACEA Biosciences, San Diego CA) equipped with a CIM-
195 plate 16 (ACEA Biosciences, San Diego CA), which is a 16-well system in which each well is
196 composed of upper and lower chambers separated by an 8-um microporous membrane.
197 Migration/invasion was measured as the relative impedance change (cell index) across
198 microelectronic sensors integrated into the bottom of the membrane. H69 and CC-LP-1 cells
199 were infected with *H. pylori* ATCC45304 strain at MOIs of 0,1,10,50 and 100 respectively for 2
200 hours prior to the experiment, then harvested later using 0.25% trypsin-EDTA and washed with
201 medium. A total of 30,000 of H69 or CC-LP-1 cells were seeded into each well of the upper
202 chamber (UC) in serum-free media. Complete media containing 10 % serum was added the
203 lower chamber (LC) of each well. The CIM-plates was left in an incubator for 1 hour to allow
204 cell attachment, then monitored for migration/invasion over 96 hours taking a reading every 15
205 minutes. For quantification, the cell index (CI) was averaged from three independent
206 measurements at each time point (41).
207
208 **Invasion monitoring in cells exposed to *H. pylori***
209
210 The rate of cell invasion was monitored in real-time using the xCELLigence system CIM-plates.
211 Two hours prior to conducting the experiment H69 or CC-LP1 cells were infected with *H. pylori*
212 ATCC45304 strain at either MOI of 0 or 10 . The UC of the CIM plate was coated with 20%
213 solution of Matrigel™ (BD Biosciences). A total of 30,000 of H69 or CC-LP-1 cells were
214 seeded in each well of the UC in serum-free media.. H69 or CC-LP media was added to each
215 well of the LC. The CIM-plates placed at 37° C in 5% CO_2 for 60 minutes to allow cell
216 attachment. The impedance value of each well was monitored by the xCELLigence system at
217 intervals of 20 minutes for 96 hours, at which point the experiment was terminated. Invasion was
218 expressed as a CI value.
219
220 **Assessment of cell proliferation**
221
222 Cell proliferation of H69 was assessed using the xCELLigence DP system (ACEA Biosciences,
223 San Diego, CA, USA). H69 cells were fasted for 4 to 6 hours in 1:20 diluted medium that had
224 been diluted 1:20 with 50% DMEM and 50% DMEM/Ham's F12, containing 1% of PS, *i.e.*
225 0.5% FBS final concentration, as described (42, 43), then the cells were co-cultured of viable
226 bacilli of *H. bilis* for 120 min before starting the assay. H69 cells were harvested later using
227 0.25% trypsin-EDTA and washed with medium. Five thousand H69 cells were seeded on to each
228 well of the E-plate in H69 medium and cultured for 24 hours. The culture medium was removed,
229 and the cells were gently washed with 1×PBS. The PBS was replaced with serum diluted
230 medium. The cellular growth was monitored in real time with readings collected at intervals of

20 minutes for ≥60 hours. For quantification, CI was averaged from three independent measurements at each time point.

Colony forming assay in soft agar

H69 cells (10,000 cells per well) were mixed with 0.3% low melting temperature agarose (NuSieveGTG; Lonza, Walkersville, MD) in growth medium, plated on top of a solidified layer of 0.6% agarose in growth medium, in 6-well or 20 mm cell culture plates, and fed every three days (twice a week) with growth medium. After 28 days or until the colonies had established, the colonies with diameter 50 µm were counted using phase-contrast microscopy (44).

Statistical analysis

Differences in cell elongation, cell scattering, wound healing and colony formation among test and control groups were analysed by one-way ANOVA. Fold differences in mRNA levels, real time cell migration and invasion through extracellular matrix were analysed by two-way ANOVA followed by Dunnett's test for multiple comparisons. Analysis was accomplished using GraphPad Prism version 7 software (GraphPad, San Diego, CA). A P value of ≤ 0.05 was considered to be statistically significant.

Results

***H. pylori* induces epithelial to mesenchymal transition (EMT) phenotype in biliary cells**

H69 were directly exposed to increasing number of *H. pylori* at 0, 10 and 100 bacilli per H69 cell in 6 wells. After 24 hours of infection, the epithelial morphology of H69 was changed into mesenchymal phenotype characterized by cell elongation, protrusion of thread-like filopodia and loss cell-cell contact in dose dependent fashion, which implicates increasing change in cell motility. The morphological change of H69 was also supported by increasing L/W ratio of *H. pylori*-infected cells, and H69 cells were more isolated after exposure to *H. pylori*, in dose-dependent fashion (Figure 2).This phenotype change can resemble the phenomenon found in AGS cell line after exposure to *H. pylori* called "Hummingbird phenotype"(Figure 1). On the other side, H69 treated with 5 ng of TGF-beta were surprisingly increased cell aggregation and nodule formation (Supplementary Figure 6).

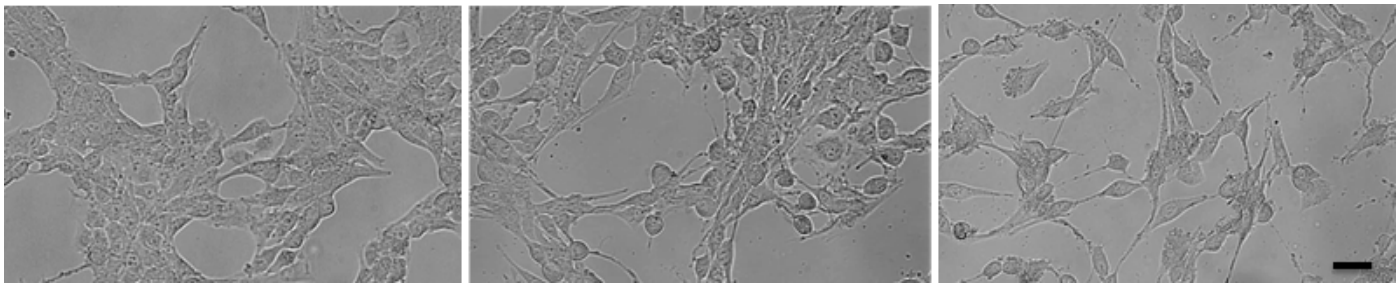

Figure 1. CagA$^+$ *H. pylori* ATCC 43504 induced phenotypic changes in cultured cholangiocytes. The photomicrographs showed cell morphology by light microscopy of H69 cells exposed to increasing numbers of *H. pylori* at 0, 10 and 100 bacteria per cholangiocyte, respectively (left to right) (A). The appearance of cells had changed from epithelial to

271 mesenchymal phenotype including loss of cell-cell contact, elongated and spindle-shaped
272 morphology along with growth as individual cells after 24 hours of *H. pylori* infection in dose-
273 dependent manner. Scale bars, 50 µm (right), 20× magnification.
274
275 **Figure 2. Quantification of epidermal to mesenchymal transition induced by cagA$^+$ *H.***
276 ***pylori.*** Cell elongation was measured by length-to-width ratio and isolate single cells were
277 counted to determine cell scattering (A, B). The number of elongated cells increased in a dose-
278 dependent fashion in response to infection by *H. pylori* (C). By contrast, the number of isolate
279 individual H69 cells indicated cell scattering was also significantly increased in dose-dependent
280 fashion (D). Data are presented as the mean values with standard errors from three replications.
281 Asterisks indicates statistically significant different of *H. pylori*-infected group compared to
282 normal group at 24 hours (*, P <0.05; **,P <0.005; ***, P <0.001; P <0.0001).

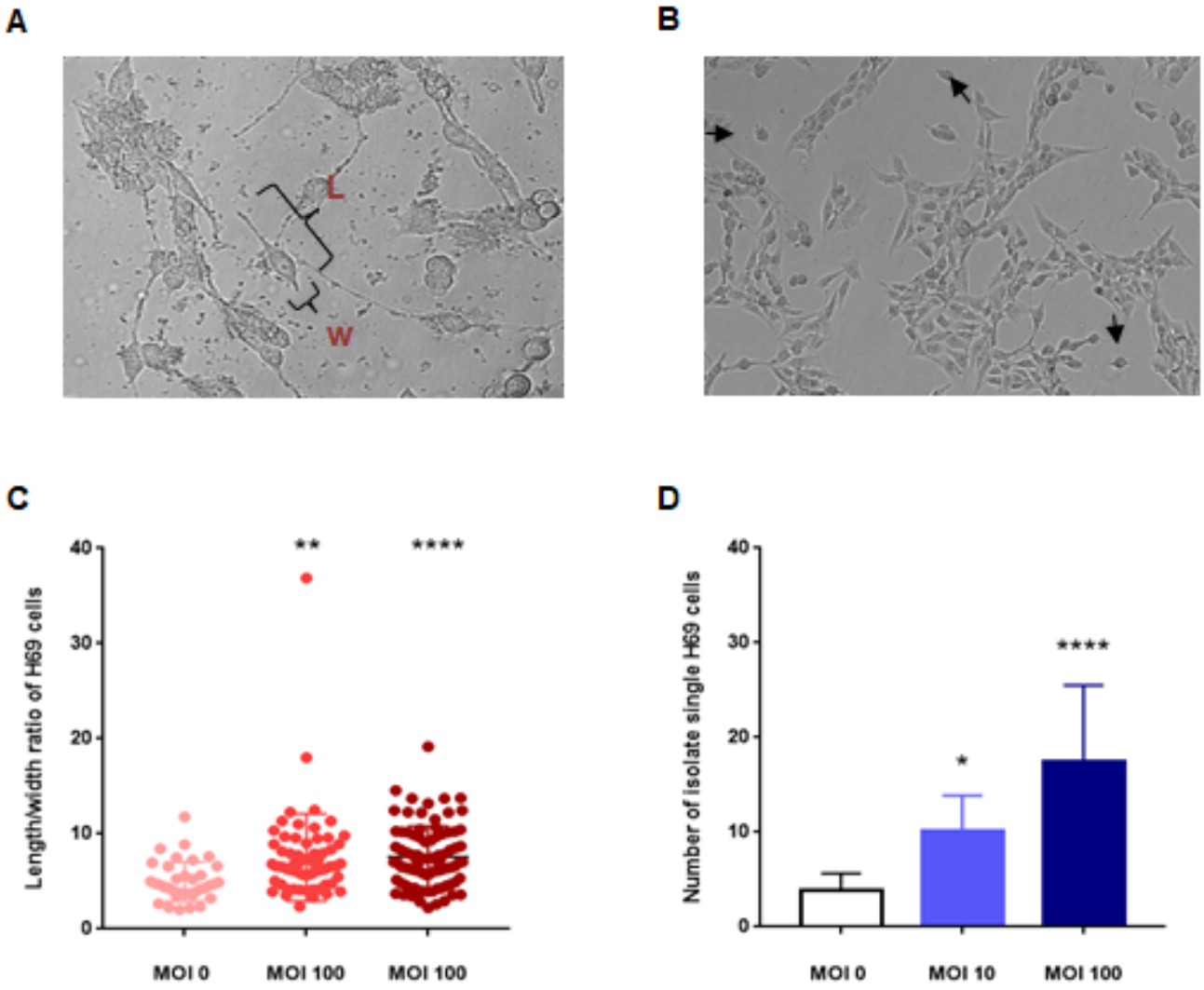

283
284
285

286 **Expression of epithelial to mesenchymal transition (EMT) associated-factors induced by**
287 **exposure to *H. pylori***
288
289 The dynamic change of EMT at transcription level was determined by quantitative real-time
290 PCR of six EMT-related factors including mesenchymal marker (vimentin), transcription factors
291 (SnaiI, Slug, Zeb1), adhesion molecules (Jam1) and proteolytic enzyme (MMP7). Two cancer
292 stem cell markers, CD24 and CD44, also were included in this analysis. Levels of fold-difference
293 for each of the six markers increased in a dose-dependent fashion. The regulatory transcriptional
294 factor, Snail was remarkably up-regulated with highest level of fold difference: 88, 656 and
295 5,309 folds in MOI 10, 50 and 100 respectively followed by MMP7 expression: 15, 21, 44 folds
296 in MOI 10, 50 and 100 respectively. Slug, Zeb1, Vimentin and Jam1 expression were up-
297 regulated at several levels of bacterial infection. In addition, the cancer stem cell markers CD24
298 was down-regulated, whereas CD44 was up-regulated, displaying a $CD44^{+}$ high/$CD24^{+}$ low
299 pattern following exposure to *H. pylori* (Figure 3)

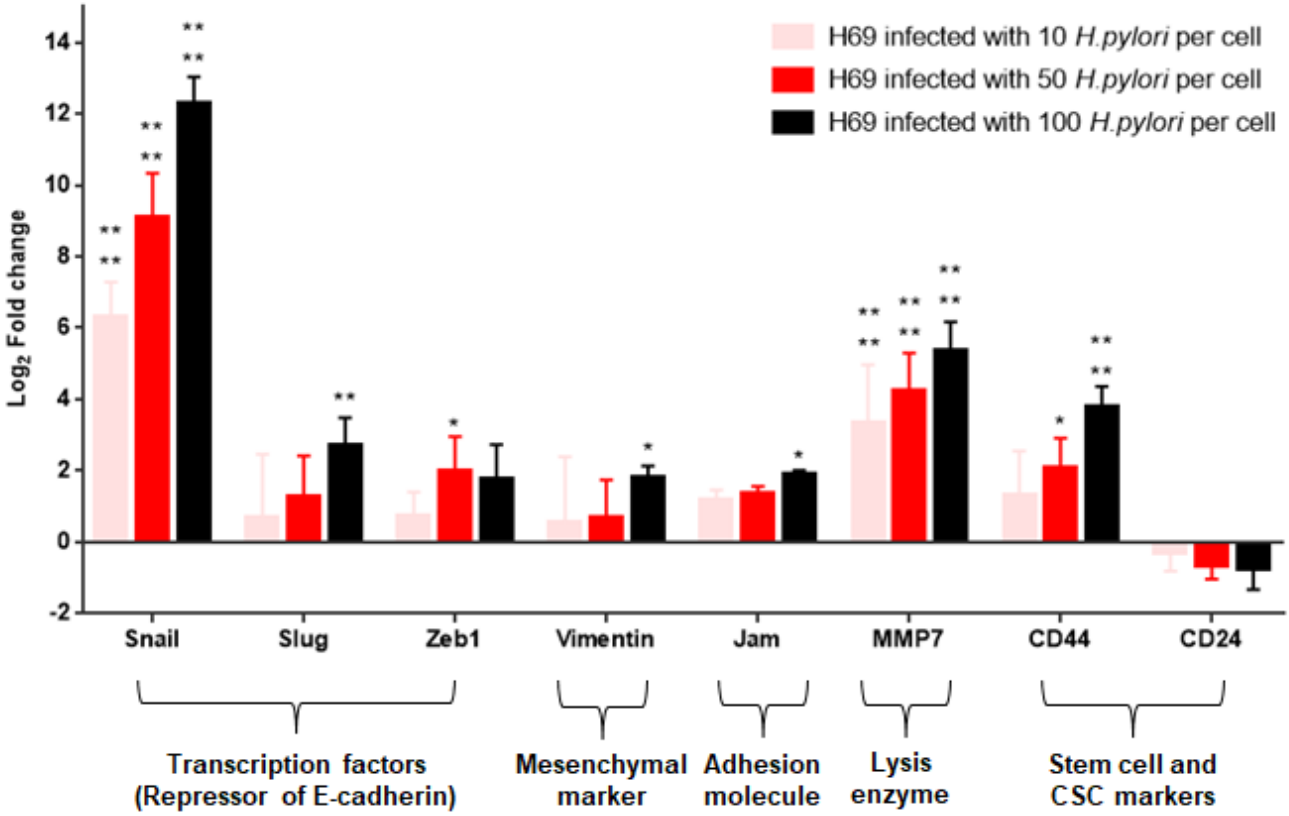

300
301 **Figure 3. Transcriptional change of EMT-related genes and cancer stem cell markers after**
302 ***H. pylori* exposure.** mRNA expression of 6 EMT-related genes and 2 cancer stem cell markers
303 were determined with three biological replicates after 24 hours of infection. Expression of Snail,
304 Slug, vimentin, Jam, MMP7 and CD44 were dose-dependently increased, whereas CD24 was
305 dose-dependently decreased. The regulatory transcriptional factor, Snail was remarkably up-
306 regulated with high level of fold difference; 88, 656 and 5,309 folds with MOI 10, 50 and 100
307 respectively. MMP7 expression was also remarkably up-regulated with every multiplicity of

infection; Slug, Zeb1, vimentin and Jam1 expression were up-regulated in specific amount of bacterial infection. The cancer stem cell markers, CD44 was significantly up-regulated with MOI 50 and 100, whereas CD24 was down-regulated. These results indicated that *H. pylori* parallelly induced EMT and stemness of Human cholangiocyte, H69. qPCR data were normalized to GAPDH expression for each sample.

Quantitative monitoring of cell migration and Matrigel invasion in real-time by xCELLigence approach

Scratch assays revealed two-dimensional migration of H69 cells. Wound healing of H69 was significantly increased to 19.47% in MOI of 10. Nevertheless, the gap closing was slowed down to 11.09% by MOI of 100 compared with healthy H69 at 14.47% (Supplementary Figure 7). Analysis in real time using the xCELLigence approach revealed that exposure to 10 to 50 *H. pylori* but not 100 *H. pylori* stimulated migration of H69 and the CC-LP1, cell line derived from a human cholangiocarcinoma, and invasion of Matrigel extracellular matrix by cells of the CC-LP-1 cholangiocarcinoma cell line (Figure 4).

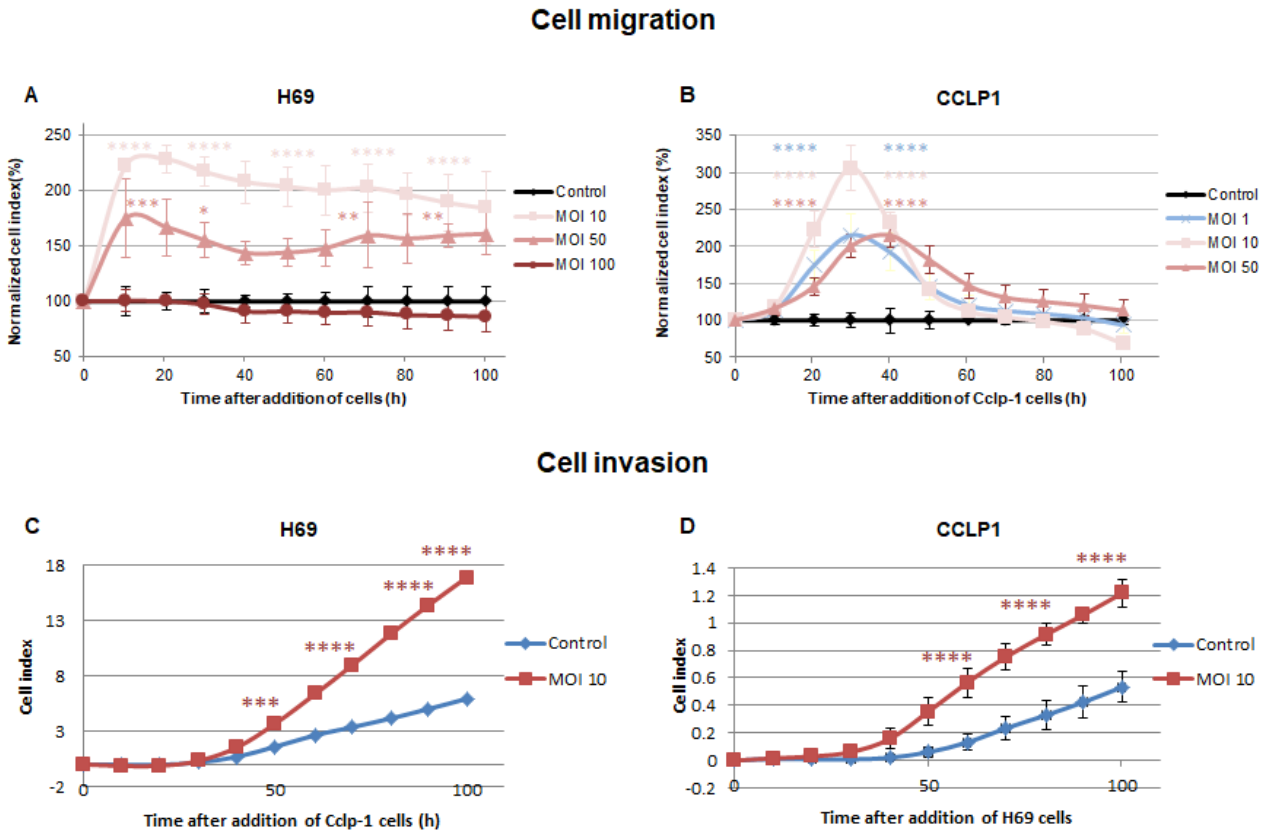

Figure 4. Investigation of EMT-associated cell behavior by Real-time cell migration and Matrigel invasion analysis using xCELLigence system. The immortalized human cholangiocyte, H69 infected with *H. pylori* showed different level of cell migratory responses

329 depending on number of infections. Group of cells infected with MOI 10 revealed the highest
330 cell migration rate followed by MOI 50, whereas MOI 100 attenuated cell migration, compared
331 with non-infected control (A). Similarly, the cholangiocarcinoma cell line, CC-LP-1 showed the
332 highest cell migration rate when stimulated with MOI 10 followed by MOI 50. Moreover, CC-
333 LP-1 cells significantly migrated faster even with 1 multiplicity of infection(B). Matrigel
334 invasion compared between MOI 10 and non-infected cells, the Invasion rate of both H69 and
335 CC-LP1 cells were significantly increased when infected with (C,D). Cell migration and invasion
336 were monitored for 100 hours with chemoattractant in the lower chamber of CIM plate.
337
338 ***H. pylori* induces contact-independent colony formation in soft agar**
339
340 The tumorigenesis of infected H69 was determined by anchorage independent cell growth in soft
341 agar. The number of colony was counted, and the results revealed that 10 multiplicity of
342 infection can significantly increase the number of colony in soft agar, but not 50 or 100 MOI.
343 The size of colonies were also increased in all infected group, but significant only in MOI of 50
344 (Supplementary Figure 3). The other species of *Helicobacter*, *H. bilis* which naturally lives in
345 the bile duct surprisingly decreased the number of colony formation in soft agar (Figure 5). The
346 inhibition effect of *H. bilis* to biliary cell proliferation was supported by real-time cell
347 proliferation approach (Supplementary Figure 4).

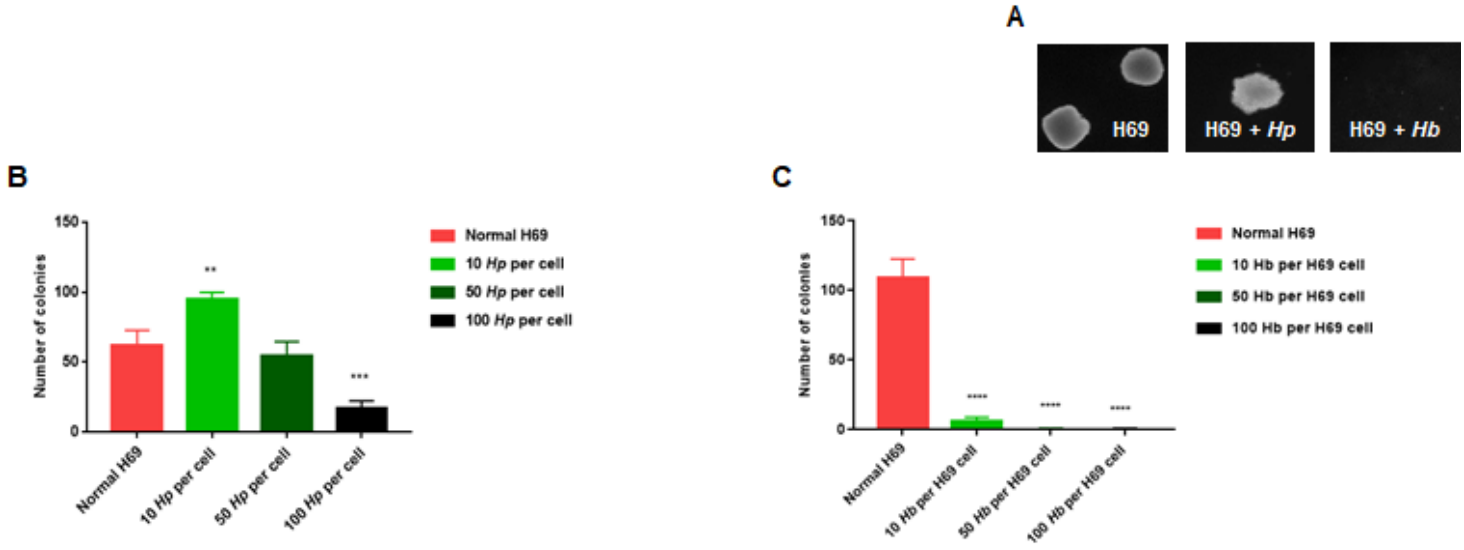

348
349
350 **Figure 5. Anchorage independent cell growth in soft agar revealed cell transformation of**
351 **H69.** Single cell of and- Infected H69 had gradually grown into colony in soft agar. Colony
352 formation was shown and counted at day 30 (A). In-infected group, number of colonies were
353 significantly increased with a MOI of 10; no different with MOI of 50; decreased with MOI of
354 100, compared with non-infected control (B). On the other side, number of colonies in infected
355 group had dramatically decreased in dose-dependent fashion, which indicated inhibitory effect of
356 this bacteria toward anchorage independent cell growth or cell transformation of H69 (C). Three
357 biological replicates of this assay were undertaken.
358

359 **Discussion**
360
361 Numerous species of *Helicobacter* have been described (45) while *H. pylori* was the first
362 bacterial pathogen confirmed to cause gastric disease including peptic ulcer, gastric lymphoma
363 and gastric adenocarcinoma (31, 46-49). Bacilli of *H. pylori* occur in the stomach in at least half
364 the human population. Transmission from mother to child and by other routes takes place. The
365 human-*H. pylori* association may be beneficial in early life, including contributions to a healthy
366 microbiome and reduced early-onset asthma (50, 51). Many strains of *H. pylori* have been
367 characterized at the molecular level, and these are generally classified as either CagA positive or
368 CagA negative. The major virulence factor, cytotoxin-associated gene A (CagA) is a ~140 kDa
369 protein encoded on the cag pathogenicity island (PAI). Cag PAI also encodes a type 4 secretion
370 channel through which the CagA virulence factor is introduced into the host cell upon attachment
371 by the bacillus (22). CagA locates to the cell membrane, from where it is phosphylorated by the
372 Src kinases. Downstream of these modifications, the activated CagA orchestrates changes in
373 morphology of the infected epithelial cell, which loses cell polarity and becomes motile,
374 exhibiting a diagnostic 'hummingbird-like' phenotype (52-54). In addition to the well-known
375 association with gastric cancer, *H. pylori* has also been associated with hepatological disease
376 including in the biliary tract (7, 8, 55). The related species, *H. hepaticus* and *H. bilis*, also have
377 been associated with hepatobiliary disease (55-57).
378
379 Infection with the fish-borne liver flukes *Opisthorchis viverrini, Clonorchis sinensis* as well as
380 the bacterial infection with *Helicobacter pylori* are all classified as Group 1 carcinogens by the
381 International Agency for Research on Cancer of the World Health Organization (9).
382 Opisthorchiasis is a major risk factor for cholangiocarcinoma in the northern and northeastern
383 part of Thailand and Laos (9-12). In addition to gastric disease, infection with species of
384 *Helicobacter* causes hepatobiliary tract diseases that can resemble opisthorchiasis (8, 14, 15) (16,
385 17). Liver fluke infection can induce lesions in biliary system including cholangitis, biliary
386 hyperplasia and metaplasia, periductal fibrosis and CCA. These lesions derive not only from
387 liver fluke infection but perhaps are in part the consequence of hepatobiliary tract infection with
388 *H. pylori*. Given the high incidence rate of cholangiocarcinoma in this endemic area where the
389 infection with *O. viverrini* prevails, and given evidence of this liver fluke as a reservoir host of
390 *H. pylori*, these two biological carcinogens may together drive the pathogenesis of
391 opisthorchiasis and cholangiocarcinoma in this region. In addition, the virulence factors of *H.*
392 *pylori* may be a key risk factor that underlie biliary tract disease including CCA during
393 opisthorchiasis (13). Furthermore, the CagA oncoprotein secreted by *H. pylori* into epithelial
394 cells is noted for its variation at the SHP2 binding site and, based on the sequence variation, is
395 subclassified into two main types - East-Asian CagA and Western CagA. East-Asian CagA
396 shows stronger SHP2 binding and greater biological activity than Western CagA. It has been
397 proposed that in East Asia, the circulation of *H. pylori* strains encoding active forms of CagA
398 underlie the elevated incidence of gastric adenocarcinoma (22).
399
400 Here, we investigated interactions among a human cholangiocyte cell line, H69, a CCA cell line
401 CC-LP-1, CagA$^+$ve *Helicobacter pylori*, and *H. bilis* bacilli.. Infection of H69 with CagA$^+$ *H.*
402 *pylori* induced epithelial to mesenchymal transition phenotype in dose-dependent manner, which
403 was characterized by cell elongation and scattering which implicate increasing change in cell
404 motility. This phenotype of H69-infected cells was reminiscent of the modified appearance of the

405 AGS gastric carcinoma cell after exposure *H. pylori*, which has been termed the hummingbird
406 phenotype (58). In AGS cells, delivery of CagA by the type IV secretion mechanism from *H.*
407 *pylori* to the epithelial cell subverts the normal signaling leading to actin-dependent
408 morphological rearrangement and the hummingbird appearance. The hitherto uniform polygonal
409 shape becomes markedly elongated with terminal needle-like projections (59).
410
411 Earlier studies in AGS cells infected with *H. pylori* had also demonstrated that the hummingbird
412 phenotype was accompanied early on with transcription changes that reflected the epithelial to
413 mesenchymal transition, EMT. Similar transcriptional changes were seen in the *H. plyori*-
414 infected H69 cells. Specifically, upregulation of expression of Snai1, Slug, vimentin, Jam1, and
415 MMP7 expression in dose-dependent fashion strongly supported, at the expression level, a
416 dynamic change in cholangiocyte reflective of EMT. Moreover, the E-cadherin repressor, Snail
417 was markedly up-regulated, which indicated that this factor may be a key driver of epithelial to
418 mesenchymal transition in H69. CD44 expression was up-regulated in dose-dependent fashion,
419 whereas CD24 decreased, showing a CD44 high/CD24 low phenotype during infection. These
420 results indicated that *H. pylori* may not only induce EMT but also contributes to stemness and
421 malignant transformation of the cholangiocyte.
422
423 Realtime cell monitoring approach by xCELLigence revealed that the H69 and CC-LP-1 cells
424 showed higher cell migration when exposed to *H. pylori*. The fastest migratory rate was MOI of
425 10 followed by MOI of 50. By contrast, the rate decreased with 100 bacteria per cell, suggested
426 direct detrimental effect of the elevated levels of bacterial exposure. Ten bacilli per cell stimulate
427 both migration and invasion of the basement membrane model matrix by both the H69 and CC-
428 LP-1 cells, which was evidence of behavioral changes in these epithelial cells characteristic of
429 epidermal to mesenchymal transition. In addition, following exposure to *H. pylori*, H69 cells
430 showed anchorage independent cell growth in soft agar, an accepted in vitro phenotype of the
431 escape from anoikosis that is characteristic of metastasis (60). At a MOI of 10, there was a
432 significant increase in numbers of colonies of the H69 cell in soft agar. By contrast, not only
433 were increase in colonies also seen after exposure of H69 cells to *H. bilis* in the model of contact
434 independent cell growth, and also cell proliferation as quantified in E-plate on the xCELLIgene
435 platform, both numbers of colonies and cell growth decreased. In general, these outcome
436 indicated that *H. pylori* has the potential to induce carcinogenic changes in cholangiocytes.
437
438 *H. pylori*-specific DNA sequences has been detected in CCA tumors and also from lesions
439 diagnosed as cholecystitis/cholelithiasis in regions endemic for opisthorchiasis (8, 14).
440 Moreover, serological findings indicate infection with *H. pylori* in Thais at high risk for CCA
441 (15). Given that here we have observed that CagA+ *H. pylori* stimulated epithelial to
442 mesenchymal transition of the human cholangiocyte which in turn indicates the underlying
443 mechanism of tissue fibrosis(61-63) and cancer metastasis(64-66) , an explanation for why
444 infection with the liver fluke induces bile duct cancer (67) might now be clearer – involvement
445 by *H. pylori* and its virulence factors. *Helicobacter* likely passes from the stomach to the
446 duodenum and enters the biliary tree through the duodenal papilla and ampulla of Vater (19, 68).
447
448 In contrast to the malignancy-conducive focus of this relationship between the liver fluke *O.*
449 *viverrini* and *H. pylori*, co-infections with *H. pylori* and other *Helicobacter* species and other
450 helminths have generally described diminution in risk for *H. pylori*-associated gastric carcinoma

451 (69-71) For example, the concurrent infection on mice with an intestinal nematode modulates
452 inflammation, induces a Th2-polarizing cytokine phenotype with concurrent downmodulation of
453 Th1 responses and the gastric immune responses, and reduces *Helicobacter*-induced gastric
454 atrophy (72). To conclude, infection with $CagA^+$ *H. pylori* induced epithelial to mesenchymal
455 transition in human cholangiocytes, along with other changes strongly reflective of malignant
456 transformation. Further investigation of the relationship of *O. viverrini* and *H. pylori* within the
457 infected biliary tract clearly is warranted.
458
459
460 **Abbreviations** Cytotoxin-associated gene A (*cag*A), cholangiocarcinoma (CCA); CagA
461 multimerization motif (CM); EMT, epithelial to mesenchymal transition; ZEB, zinc finger E-
462 box-binding homeobox 1; VIM, vimentin; SNAII, MMP7 and cancer stem cell marker CD44;
463 CD24.
464
465 **Competing Financial Interests**
466
467 The authors declare there were no competing financial interests.
468
469 **Acknowledgments**
470
471 We thank Dr. James G. Fox for advice and cultures of *H. bilis* and related bacilli. P.T.
472 acknowledges support as a PhD research scholar from the Thailand Research Fund under the
473 Royal Golden Jubilee scholars program (grant number PHD/0013/2555); B.S. acknowledges
474 support from Thailand Research Fund Senior Research Scholar. This work was supported by the
475 National Health Security Office, Thailand, the Higher Education Research Promotion and
476 National Research University Project of Thailand, Office of the Higher Education Commission,
477 through the Health Cluster (SHeP-GMS), the Faculty of Medicine, Khon Kaen University,
478 Thailand (award number I56110), and the Thailand Research Fund under the TRF Senior
479 Research Scholar (RTA 5680006); the National Research Council of Thailand. The National
480 Institute of Allergy and Infectious Diseases (NIAID), Tropical Medicine Research Center award
481 number P50AI098639, The National Cancer Institute, award number R01CA164719, and the
482 United States Army Medical Research and Materiel Command (USAMRMC), contract number
483 W81XWH-12-C-0267 also provided support. The content is solely the responsibility of the
484 authors and does not necessarily represent the official views of the funders including
485 USAMRMC, NIAID, NCI or the NIH.
486
487 **Author contributions**
488
489 P.T., S.S. C.P., Y.C., B.S. and P.J.B. conceived and designed the study. P.T., S.K., V.M., W.I.
490 performed the experiments. J.F. provides H. bilis and experimental designs. P.T., W.I., B.S., J.F.
491 and PJB analyzed and interpreted the findings. P.T., B.S., W.I., S.S., and PJB wrote the
492 manuscript. All authors read and approved the final version of the paper.
493
494

495

496

497

498 **Supporting information**

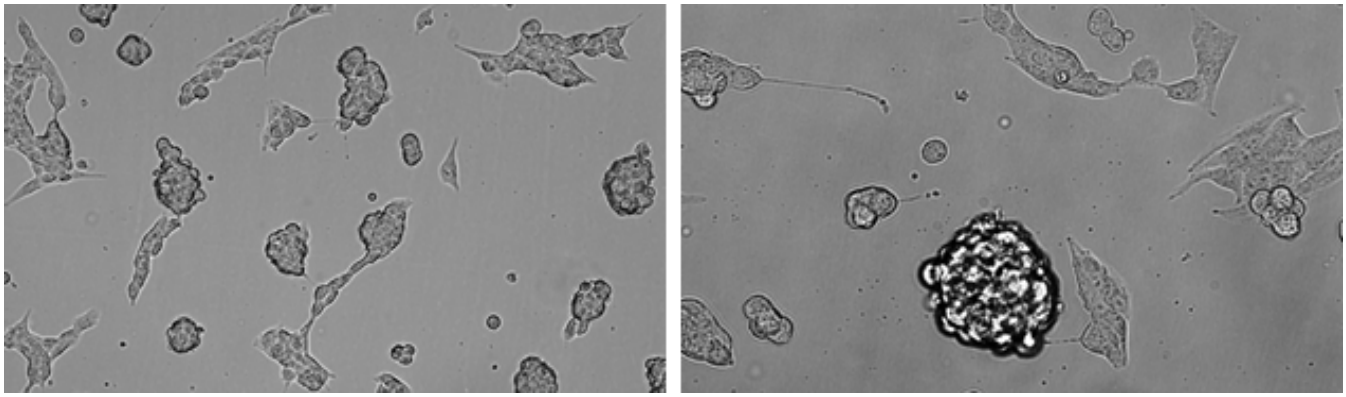

499

500 **Supplementary Figure 1. TGF-Beta promoted nodule formation.** TGF-beta (EMT
501 stimulating agent) induced nodule formation in the human cholangiocyte cell line, H69. Cells
502 were cultured in the presence of 5 ng/ml TGF-beta in serum and hormone-free media for 24
503 hours.
504
505
506

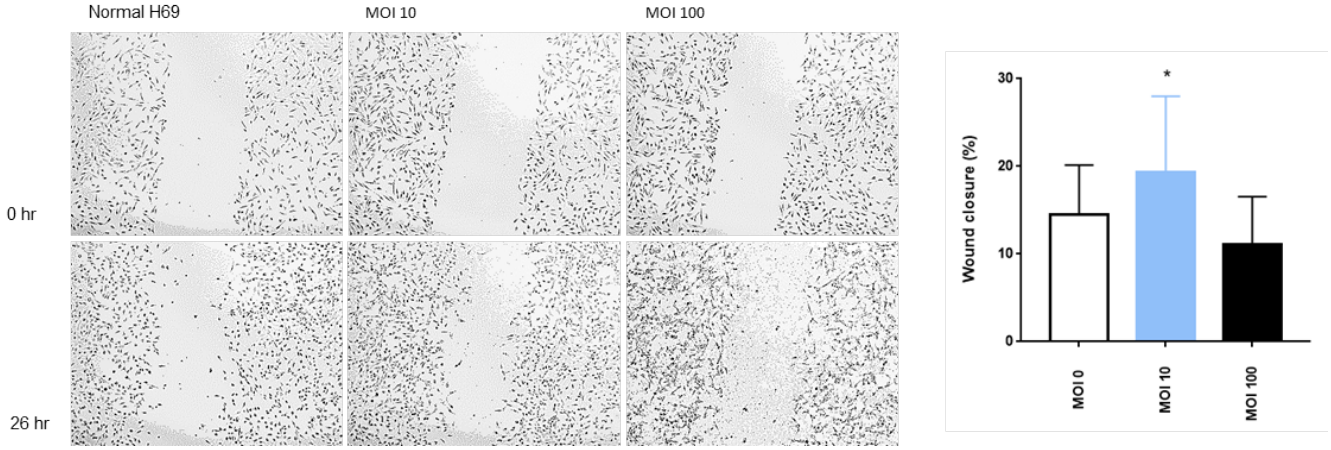

507
508
509

510 **Supplementary Figure 2. Wound healing revealed cell migration of H69 cholangiocytes**
511 **infected with *Helicobacter pylori* in two dimensions.** To investigate the effect of on cell
512 migration, the scratch assay was performed in triplicate with different number of bacterial
513 infections. Wound closure was significantly increased to 19.47% with a MOI 10 of *H. pylori*.
514 Nevertheless, MOI 100 showed lower cell migration at 11.09%, compared with control at
515 14.47%. The photomicrograph at 0 and 26 hours, 5×magnification.

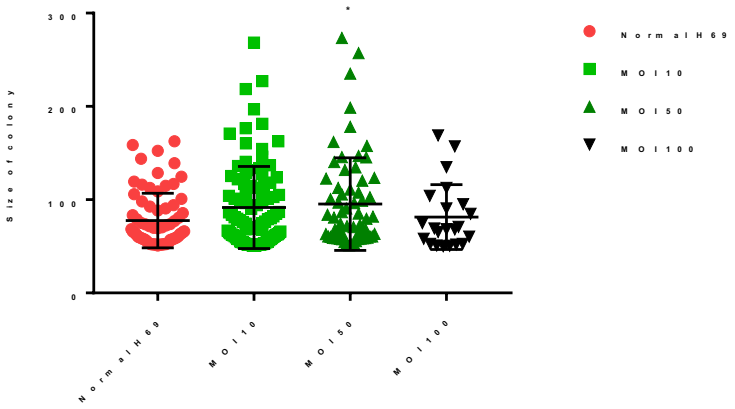

516
517
518 **Supplementary Figure 3. Size of colony in soft agar.** The colonies with diameter over 50 µm
519 were measure and calculated. The average size of colonies were 77.63, 91.62, 95.25 and 81.46
520 µm in MOI 0f 0, 10, 50 and 100, respectively.
521
522

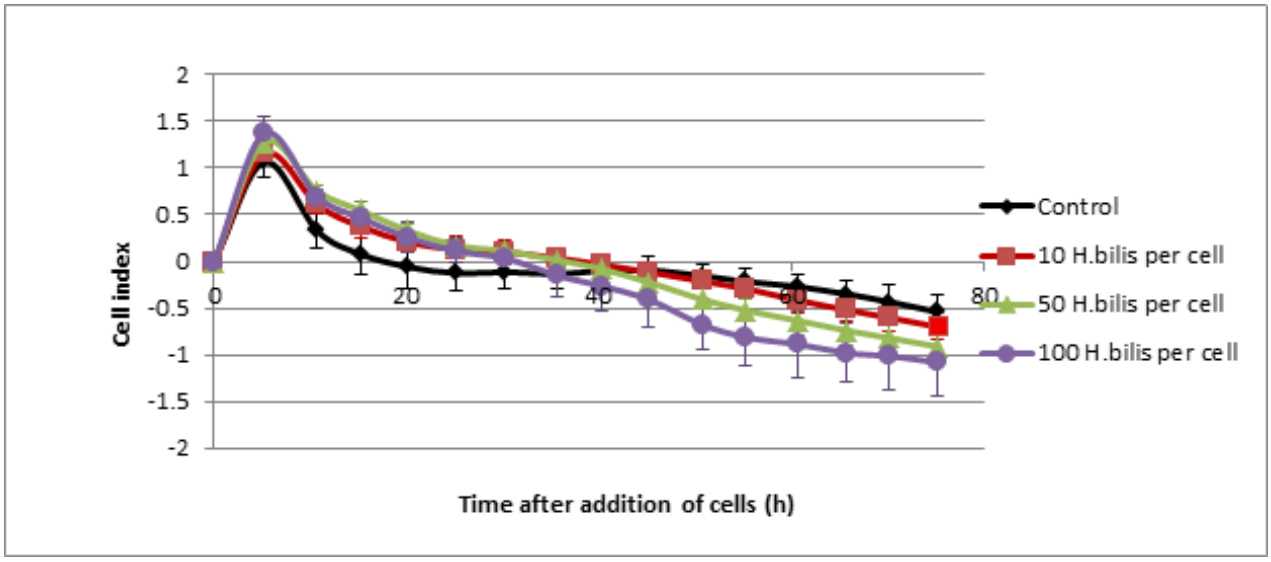

523
524

525 **Supplementary Figure 4. Real time cell proliferation of-infected H69 determined by**
526 **xCELLigence approach.** The immortalized human cholangiocyte, H69 cells were infected with
527 increasing number of (ATCC 43879) at MOI 10, 50 and 100, respectively. Cell growth indicated
528 by cell index of all infected groups were dramatically decreased and lower than control after 40
529 hours. MOI 100 had the lowest cell proliferation followed by MOI 50 and MOI 10 respectively.
530 The results indicated cell growth inhibitory effect of toward H69. Cells proliferation assay were
531 performed in E-plate in minimal media.
532
533

Gene name	Gen Bank Number	Primer sequence (5'-3')	Product size (bp)
CD24	NM_013230.3	Forward CACCCAGCATCCTGCTAGAC Reverse GAGACCACGAAGAGACTGGC	259
CD44	NM_00610.3	Forward GGGAGTCAAGAAGGTGGAGC Reverse CTGAGACTTGCTGGCCTCTC	237
F11r/Jam1	NM_016946.5	Forward GTGCCTACTCGGGCTTTTCT Reverse GAGCTTGACCTTGACCTCCC	201
Gapdh	NM_002046.5	Forward CCCATGTTCGTCATGGGTGT Reverse TTCTAGACGGCAGGTCAGGT	366
MMP7	NM_002423.5	Forward GGAGCTCATGGGGACTCCTA Reverse GGCCAAGTTCATGAGTTGCAG	172
Snai1	NM_005985.3	Forward AGCTCTCTGAGGCCAAGGAT Reverse GACATTCGGGAGAAGGTCCG	325
Vimentin	NM_003380.5	Forward GCAGGAGGCAGAAGAATGGT Reverse GCAGCTTCAACGGCAAAGTT	216
Zeb1	NM_001128128.2	Forward CGCAGTCTGGGTGTAATCGT Reverse CCATGCCCTGAGGAGAACTG	477

534
535
536 **Supplementary Table 1. Nucleotide sequences of primers specific for EM- associated**
537 **human genes, which were used in |quantitative real-time PCR analysis.**

538
539
540
541
542
543
544
545
546
547
548
549
550
551
552
553

554 **References**
555
556 1. McNulty SN, Tort JF, Rinaldi G, Fischer K, Rosa BA, Smircich P, et al. Genomes of
557 Fasciola hepatica from the Americas Reveal Colonization with Neorickettsia Endobacteria
558 Related to the Agents of Potomac Horse and Human Sennetsu Fevers. PLoS Genet.
559 2017;13(1):e1006537.
560 2. Van CD, Doungchawee G, Suttiprapa S, Arimatsu Y, Kaewkes S, Sripa B. Association
561 between Opisthorchis viverrini and Leptospira spp. infection in endemic Northeast Thailand.
562 Parasitol Int. 2017;66(4):503-9.
563 3. Gendrel D, Kombila M, Beaudoin-Leblevec G, Richard-Lenoble D. Nontyphoidal
564 salmonellal septicemia in Gabonese children infected with Schistosoma intercalatum. Clin Infect
565 Dis. 1994;18(1):103-5.
566 4. Deenonpoe R, Chomvarin C, Pairojkul C, Chamgramol Y, Loukas A, Brindley PJ, et al.
567 The carcinogenic liver fluke Opisthorchis viverrini is a reservoir for species of Helicobacter.
568 Asian Pac J Cancer Prev. 2015;16(5):1751-8.
569 5. Deenonpoe R, Mairiang E, Mairiang P, Pairojkul C, Chamgramol Y, Rinaldi G, et al.
570 Elevated prevalence of Helicobacter species and virulence factors in opisthorchiasis and
571 associated hepatobiliary disease. Sci Rep. 2017;7:42744.
572 6. Sripa B, Deenonpoe R, Brindley PJ. Co-infections with liver fluke and Helicobacter
573 species: A paradigm change in pathogenesis of opisthorchiasis and cholangiocarcinoma?
574 Parasitol Int. 2017;66(4):383-9.
575 7. Boonyanugomol W, Chomvarin C, Song JY, Kim KM, Kim JM, Cho MJ, et al. Effects of
576 Helicobacter pylori gamma-glutamyltranspeptidase on apoptosis and inflammation in human
577 biliary cells. Dig Dis Sci. 2012;57(10):2615-24.
578 8. Boonyanugomol W, Chomvarin C, Sripa B, Bhudhisawasdi V, Khuntikeo N,
579 Hahnvajanawong C, et al. Helicobacter pylori in Thai patients with cholangiocarcinoma and its
580 association with biliary inflammation and proliferation. HPB (Oxford). 2012;14(3):177-84.
581 9. Humans IWGotEoCRt. Biological agents. Volume 100 B. A review of human
582 carcinogens. IARC Monogr Eval Carcinog Risks Hum. 2012;100(Pt B):1-441.
583 10. Sungkasubun P, Siripongsakun S, Akkarachinorate K, Vidhyarkorn S, Worakitsitisatorn
584 A, Sricharunrat T, et al. Ultrasound screening for cholangiocarcinoma could detect premalignant
585 lesions and early-stage diseases with survival benefits: a population-based prospective study of
586 4,225 subjects in an endemic area. BMC Cancer. 2016;16:346.
587 11. Khuntikeo N, Loilome W, Thinkhamrop B, Chamadol N, Yongvanit P. A Comprehensive
588 Public Health Conceptual Framework and Strategy to Effectively Combat Cholangiocarcinoma
589 in Thailand. PLoS Negl Trop Dis. 2016;10(1):e0004293.
590 12. Aye Soukhathammavong P, Rajpho V, Phongluxa K, Vonghachack Y, Hattendorf J,
591 Hongvanthong B, et al. Subtle to severe hepatobiliary morbidity in Opisthorchis viverrini
592 endemic settings in southern Laos. Acta Trop. 2015;141(Pt B):303-9.
593 13. Segura-Lopez FK, Guitron-Cantu A, Torres J. Association between Helicobacter spp.
594 infections and hepatobiliary malignancies: a review. World J Gastroenterol. 2015;21(5):1414-23.
595 14. Boonyanugomol W, Chomvarin C, Sripa B, Chau-In S, Pugkhem A, Namwat W, et al.
596 Molecular analysis of Helicobacter pylori virulent-associated genes in hepatobiliary patients.
597 HPB (Oxford). 2012;14(11):754-63.
598 15. Pisani P, Whary MT, Nilsson I, Sriamporn S, Wadstrom T, Fox JG, et al. Cross-reactivity
599 between immune responses to Helicobacter bilis and Helicobacter pylori in a population in

600 Thailand at high risk of developing cholangiocarcinoma. Clin Vaccine Immunol.
601 2008;15(9):1363-8.
602 16. Lvova MN, Tangkawattana S, Balthaisong S, Katokhin AV, Mordvinov VA, Sripa B.
603 Comparative histopathology of Opisthorchis felineus and Opisthorchis viverrini in a hamster
604 model: an implication of high pathogenicity of the European liver fluke. Parasitol Int.
605 2012;61(1):167-72.
606 17. Mairiang E, Laha T, Bethony JM, Thinkhamrop B, Kaewkes S, Sithithaworn P, et al.
607 Ultrasonography assessment of hepatobiliary abnormalities in 3359 subjects with Opisthorchis
608 viverrini infection in endemic areas of Thailand. Parasitol Int. 2012;61(1):208-11.
609 18. Plieskatt JL, Deenonpoe R, Mulvenna JP, Krause L, Sripa B, Bethony JM, et al. Infection
610 with the carcinogenic liver fluke Opisthorchis viverrini modifies intestinal and biliary
611 microbiome. FASEB J. 2013;27(11):4572-84.
612 19. Boonyanugomol W, Chomvarin C, Hahnvajanawong C, Sripa B, Kaparakis-Liaskos M,
613 Ferrero RL. Helicobacter pylori cag pathogenicity island (cagPAI) involved in bacterial
614 internalization and IL-8 induced responses via NOD1- and MyD88-dependent mechanisms in
615 human biliary epithelial cells. PLoS One. 2013;8(10):e77358.
616 20. Hatakeyama M. Helicobacter pylori CagA and gastric cancer: a paradigm for hit-and-run
617 carcinogenesis. Cell Host Microbe. 2014;15(3):306-16.
618 21. Lamouille S, Xu J, Derynck R. Molecular mechanisms of epithelial-mesenchymal
619 transition. Nat Rev Mol Cell Biol. 2014;15(3):178-96.
620 22. Hatakeyama M. Oncogenic mechanisms of the Helicobacter pylori CagA protein. Nat
621 Rev Cancer. 2004;4(9):688-94.
622 23. Fox JG. Helicobacter bilis: bacterial provocateur orchestrates host immune responses to
623 commensal flora in a model of inflammatory bowel disease. Gut. 2007;56(7):898-900.
624 24. Grubman SA, Perrone RD, Lee DW, Murray SL, Rogers LC, Wolkoff LI, et al.
625 Regulation of intracellular pH by immortalized human intrahepatic biliary epithelial cell lines.
626 Am J Physiol. 1994;266(6 Pt 1):G1060-70.
627 25. Park J, Gores GJ, Patel T. Lipopolysaccharide induces cholangiocyte proliferation via an
628 interleukin-6-mediated activation of p44/p42 mitogen-activated protein kinase. Hepatology.
629 1999;29(4):1037-43.
630 26. Shimizu Y, Demetris AJ, Gollin SM, Storto PD, Bedford HM, Altarac S, et al. Two new
631 human cholangiocarcinoma cell lines and their cytogenetics and responses to growth factors,
632 hormones, cytokines or immunologic effector cells. Int J Cancer. 1992;52(2):252-60.
633 27. Bairoch A. The Cellosaurus, a Cell-Line Knowledge Resource. J Biomol Tech.
634 2018;29(2):25-38.
635 28. Han C, Demetris AJ, Michalopoulos GK, Zhan Q, Shelhamer JH, Wu T. PPARgamma
636 ligands inhibit cholangiocarcinoma cell growth through p53-dependent GADD45 and p21
637 pathway. Hepatology. 2003;38(1):167-77.
638 29. Smout MJ, Sotillo J, Laha T, Papatpremsiri A, Rinaldi G, Pimenta RN, et al.
639 Carcinogenic Parasite Secretes Growth Factor That Accelerates Wound Healing and Potentially
640 Promotes Neoplasia. PLoS Pathog. 2015;11(10):e1005209.
641 30. Arunsan P, Ittiprasert W, Smout MJ, Cochran CJ, Mann VH, Chaiyadet S, et al.
642 Programmed knockout mutation of liver fluke granulin attenuates virulence of infection-induced
643 hepatobiliary morbidity. Elife. 2019;8.
644 31. Marshall BJ, Warren JR. Unidentified curved bacilli in the stomach of patients with
645 gastritis and peptic ulceration. Lancet. 1984;1(8390):1311-5.

646 32. Dewhirst FE, Fox JG, Mendes EN, Paster BJ, Gates CE, Kirkbride CA, et al. 'Flexispira
647 rappini' strains represent at least 10 Helicobacter taxa. Int J Syst Evol Microbiol. 2000;50 Pt
648 5:1781-7.
649 33. Fox JG, Yan LL, Dewhirst FE, Paster BJ, Shames B, Murphy JC, et al. Helicobacter bilis
650 sp. nov., a novel Helicobacter species isolated from bile, livers, and intestines of aged, inbred
651 mice. J Clin Microbiol. 1995;33(2):445-54.
652 34. Hachem CY, Clarridge JE, Evans DG, Graham DY. Comparison of agar based media for
653 primary isolation of Helicobacter pylori. J Clin Pathol. 1995;48(8):714-6.
654 35. Jung SW, Thamphiwatana S, Zhang L, Obonyo M. Mechanism of antibacterial activity of
655 liposomal linolenic acid against Helicobacter pylori. PLoS One. 2015;10(3):e0116519.
656 36. Lin SN, Ayada K, Zhao Y, Yokota K, Takenaka R, Okada H, et al. Helicobacter pylori
657 heat-shock protein 60 induces production of the pro-inflammatory cytokine IL8 in monocytic
658 cells. J Med Microbiol. 2005;54(Pt 3):225-33.
659 37. Pan H, Zhang Y, He GX, Katagori N, Chen H. A comparison of conventional methods
660 for the quantification of bacterial cells after exposure to metal oxide nanoparticles. BMC
661 Microbiol. 2014;14:222.
662 38. Bindschadler M, McGrath JL. Sheet migration by wounded monolayers as an emergent
663 property of single-cell dynamics. J Cell Sci. 2007;120(Pt 5):876-84.
664 39. Liang CC, Park AY, Guan JL. In vitro scratch assay: a convenient and inexpensive
665 method for analysis of cell migration in vitro. Nat Protoc. 2007;2(2):329-33.
666 40. Livak KJ, Schmittgen TD. Analysis of relative gene expression data using real-time
667 quantitative PCR and the 2(-Delta Delta C(T)) Method. Methods. 2001;25(4):402-8.
668 41. Xie H, Lee L, Scicluna P, Kavak E, Larsson C, Sandberg R, et al. Novel functions and
669 targets of miR-944 in human cervical cancer cells. Int J Cancer. 2015;136(5):E230-41.
670 42. Matchimakul P, Rinaldi G, Suttiprapa S, Mann VH, Popratiloff A, Laha T, et al.
671 Apoptosis of cholangiocytes modulated by thioredoxin of carcinogenic liver fluke. Int J Biochem
672 Cell Biol. 2015;65:72-80.
673 43. Rinaldi G, Yan H, Nacif-Pimenta R, Matchimakul P, Bridger J, Mann VH, et al.
674 Cytometric analysis, genetic manipulation and antibiotic selection of the snail embryonic cell
675 line Bge from Biomphalaria glabrata, the intermediate host of Schistosoma mansoni. Int J
676 Parasitol. 2015;45(8):527-35.
677 44. Horibata S, Vo TV, Subramanian V, Thompson PR, Coonrod SA. Utilization of the Soft
678 Agar Colony Formation Assay to Identify Inhibitors of Tumorigenicity in Breast Cancer Cells. J
679 Vis Exp. 2015(99):e52727.
680 45. Flahou B, Rimbara E, Mori S, Haesebrouck F, Shibayama K. The Other Helicobacters.
681 Helicobacter. 2015;20 Suppl 1:62-7.
682 46. Cover TL. Helicobacter pylori Diversity and Gastric Cancer Risk. MBio.
683 2016;7(1):e01869-15.
684 47. Marshall BJ. The pathogenesis of non-ulcer dyspepsia. Med J Aust. 1985;143(7):319.
685 48. Gaynor EC, Szymanski CM. The 30th anniversary of Campylobacter, Helicobacter, and
686 Related Organisms workshops-what have we learned in three decades? Front Cell Infect
687 Microbiol. 2012;2:20.
688 49. Sheh A, Fox JG. The role of the gastrointestinal microbiome in Helicobacter pylori
689 pathogenesis. Gut Microbes. 2013;4(6):505-31.

690 50. Kienesberger S, Cox LM, Livanos A, Zhang XS, Chung J, Perez-Perez GI, et al. Gastric
691 Helicobacter pylori Infection Affects Local and Distant Microbial Populations and Host
692 Responses. Cell Rep. 2016;14(6):1395-407.
693 51. Cover TL, Blaser MJ. Helicobacter pylori in health and disease. Gastroenterology.
694 2009;136(6):1863-73.
695 52. Saadat I, Higashi H, Obuse C, Umeda M, Murata-Kamiya N, Saito Y, et al. Helicobacter
696 pylori CagA targets PAR1/MARK kinase to disrupt epithelial cell polarity. Nature.
697 2007;447(7142):330-3.
698 53. Hatakeyama M, Higashi H. Helicobacter pylori CagA: a new paradigm for bacterial
699 carcinogenesis. Cancer Sci. 2005;96(12):835-43.
700 54. Yamaoka Y. Mechanisms of disease: Helicobacter pylori virulence factors. Nat Rev
701 Gastroenterol Hepatol. 2010;7(11):629-41.
702 55. Murphy G, Michel A, Taylor PR, Albanes D, Weinstein SJ, Virtamo J, et al. Association
703 of seropositivity to Helicobacter species and biliary tract cancer in the ATBC study. Hepatology.
704 2014;60(6):1963-71.
705 56. Mateos-Munoz B, Perez-de-la-Serna J, Ruiz-de-Leon A, Serrano-Falcon B, Casabona-
706 Frances S, Velasco-Cerrudo A, et al. Enterohepatic Helicobacter other than Helicobacter pylori.
707 Rev Esp Enferm Dig. 2013;105(8):477-84.
708 57. Zhou D, Wang JD, Weng MZ, Zhang Y, Wang XF, Gong W, et al. Infections of
709 Helicobacter spp. in the biliary system are associated with biliary tract cancer: a meta-analysis.
710 Eur J Gastroenterol Hepatol. 2013;25(4):447-54.
711 58. Wroblewski LE, Peek RM, Jr., Wilson KT. Helicobacter pylori and gastric cancer:
712 factors that modulate disease risk. Clin Microbiol Rev. 2010;23(4):713-39.
713 59. Segal ED, Cha J, Lo J, Falkow S, Tompkins LS. Altered states: involvement of
714 phosphorylated CagA in the induction of host cellular growth changes by Helicobacter pylori.
715 Proc Natl Acad Sci U S A. 1999;96(25):14559-64.
716 60. Simpson CD, Anyiwe K, Schimmer AD. Anoikis resistance and tumor metastasis. Cancer
717 Lett. 2008;272(2):177-85.
718 61. Fragiadaki M, Mason RM. Epithelial-mesenchymal transition in renal fibrosis - evidence
719 for and against. Int J Exp Pathol. 2011;92(3):143-50.
720 62. Rout-Pitt N, Farrow N, Parsons D, Donnelley M. Epithelial mesenchymal transition
721 (EMT): a universal process in lung diseases with implications for cystic fibrosis
722 pathophysiology. Respir Res. 2018;19(1):136.
723 63. Stone RC, Pastar I, Ojeh N, Chen V, Liu S, Garzon KI, et al. Epithelial-mesenchymal
724 transition in tissue repair and fibrosis. Cell Tissue Res. 2016;365(3):495-506.
725 64. Kalluri R, Weinberg RA. The basics of epithelial-mesenchymal transition. J Clin Invest.
726 2009;119(6):1420-8.
727 65. Li L, Li W. Epithelial-mesenchymal transition in human cancer: comprehensive
728 reprogramming of metabolism, epigenetics, and differentiation. Pharmacol Ther. 2015;150:33-
729 46.
730 66. Sciacovelli M, Frezza C. Metabolic reprogramming and epithelial-to-mesenchymal
731 transition in cancer. FEBS J. 2017;284(19):3132-44.
732 67. Jurberg AD, Brindley PJ. Gene function in schistosomes: recent advances toward a cure.
733 Front Genet. 2015;6:144.
734 68. Pellicano R, Menard A, Rizzetto M, Megraud F. Helicobacter species and liver diseases:
735 association or causation? Lancet Infect Dis. 2008;8(4):254-60.

736 69. Holcombe C. Helicobacter pylori: the African enigma. Gut. 1992;33(4):429-31.
737 70. Du Y, Agnew A, Ye XP, Robinson PA, Forman D, Crabtree JE. Helicobacter pylori and
738 Schistosoma japonicum co-infection in a Chinese population: helminth infection alters humoral
739 responses to H. pylori and serum pepsinogen I/II ratio. Microbes Infect. 2006;8(1):52-60.
740 71. Whary MT, Sundina N, Bravo LE, Correa P, Quinones F, Caro F, et al. Intestinal
741 helminthiasis in Colombian children promotes a Th2 response to Helicobacter pylori: possible
742 implications for gastric carcinogenesis. Cancer Epidemiol Biomarkers Prev. 2005;14(6):1464-9.
743 72. Fox JG, Beck P, Dangler CA, Whary MT, Wang TC, Shi HN, et al. Concurrent enteric
744 helminth infection modulates inflammation and gastric immune responses and reduces
745 helicobacter-induced gastric atrophy. Nat Med. 2000;6(5):536-42.
746